Eur. Phys. J. D (2014) 68: 155
DOI: 10.1140/epjd/e2014-50090-x

THE EUROPEAN PHYSICAL JOURNAL D

Topical Review

Gas breakdown and secondary electron yields*

Dragana Marić[a], Marija Savić, Jelena Sivoš, Nikola Škoro, Marija Radmilović-Radjenović, Gordana Malović, and Zoran Lj. Petrović

Institute of Physics Belgrade, University of Belgrade, Pregrevica 118, 11080 Belgrade, Serbia

Received 31 January 2014 / Received in final form 8 April 2014
Published online 23 June 2014 – © EDP Sciences, Società Italiana di Fisica, Springer-Verlag 2014

Abstract. In this paper we present a systematic study of the gas breakdown potentials. An analysis of the key elementary processes in low-current low-pressure discharges is given, with an aim to illustrate how such discharges are used to determine swarm parameters and how such data may be applied to modeling discharges. Breakdown data obtained in simple parallel-plate geometry are presented for a number of atomic and molecular gases. Ionization coefficients, secondary electron yields and their influence on breakdown are analyzed, with special attention devoted to non-hydrodynamic conditions near cathode.

1 Introduction

It is often said that atomic and molecular collisions define the physics of non-equilibrium (so-called low-temperature) plasma. However, in plasma modeling, where space charge and field profile effects intervene with atomic and molecular collisions, often it is claimed that the collisional cross sections, rate coefficients and swarm transport data do not need to be very accurate as the processes are so complicated that high accuracy is not required. Gas breakdown, on the other hand, is the point where inaccuracies of the atomic collision and swarm data are amplified and at the same time the conditions for the breakdown often define the operating conditions for the plasma. To illustrate this we may give an example that ionization rate enters the breakdown condition in exponent and also that rate is often exponentially dependent on the gas density normalized electric field E/N. The mean energy and the shape of the distribution function that define the rate (together with the cross section for ionization) are on the other hand strongly dependent on all relevant inelastic processes. Breakdown under DC fields and slowly varying AC fields also depends on surface collisions of ions and atoms. Thus, breakdown condition is a very sensitive projection of atomic and molecular collision and swarm transport physics onto the realm of plasma physics.

Gas breakdown has been studied over 100 years and yet many open issues still remain. In DC discharges, the breakdown is usually described by the standard Townsend's theory [1]. Within the past 20 years, with development of experimental and modeling techniques, it became clear that the standard (basic Townsend's theory as depicted in the textbooks) theory of breakdown and low-current discharges (the so-called Townsend's regime) requires improvement. Phelps and coworkers [2–5] initiated a comprehensive revision of the theory in all its aspects.

This revision in the lowest current limit (breakdown) included taking into account the contribution of all feedback mechanisms and space-charge effects in breakdown and low-current discharges [5]. These authors only covered one gas (argon) with detailed analysis. This is why we felt that a survey of the existing well documented breakdown data would be of value as the basis for further study on the data and elucidation of the issues in use of secondary electron yields in plasma modeling. All of the presented results were obtained in our laboratory and an utmost care has been invested to avoid the usual problems in determining the breakdown data (often depicted as Paschen curves). Those include variable surface conditions, jumping straight into the glow discharge mode, recording the operating conditions for the glow discharge and also the uncertainties that arise from the long statistical delays in initiation of gas discharges.

For many years swarm experiments have represented the primary source of data for gas discharge modeling, which, on the other hand, was based on the transport theory for swarms. With only very few exceptions, the models are based on the hydrodynamic (in equilibrium with the electric field and spatially uniform) transport data. This is however not applicable in most breakdown experiments as the early stages of the breakdown occur before equilibration of the electron swarm. Thus we present also an analysis of electron excitation cross sections and studies of spatial profiles of emission to separate excitation by electrons and fast neutrals [6]. Our results also allow us to determine the width of the non-hydrodynamic region close to the cathode and the effective multiplication as

* Contribution to the Topical Issue "Electron and Positron Induced Processes", edited by Michael Brunger, Radu Campeanu, Masamitsu Hoshino, Oddur Ingólfsson, Paulo Limão-Vieira, Nigel Mason, Yasuyuki Nagashima and Hajime Tanuma.

[a] e-mail: draganam@ipb.ac.rs

well as the approximate determination of the field distribution in dark Townsend discharges. These data all need to be applied to determine the secondary electron yields and in modeling of plasmas.

Over the past two decades determination of the secondary electron yields [6,7] has had renewed interests, for two reasons. First, a systematic survey [5] has been made of all the processes that participate to secondary electron production and it was shown that the basic assumption of Townsend's theory that ions produce the secondary electrons is correct only in a very narrow range of conditions, while photons and gas phase ionization by neutrals contribute to the secondary electron production in a much wider range of E/N. Most importantly, it became possible to model the observed secondary electron yields in the breakdown by using binary collision (beam to surface) data.

It was shown that it is not possible to use directly the binary collision (beam-surface) data for the analysis of gas discharges and low temperature plasmas as those would have specific distributions of all the relevant fluxes that otherwise might be connected through nonlinear relations. The analysis performed for the breakdown (where all fluxes are in linear relation to the initial flux of electrons) proved to be quite robust and still fit most of the data for the glow discharges [8,9]. Nevertheless, it is possible that for some gases or some plasmas, nonlinearities may prevail and the required model may depart from the breakdown model.

In this paper we present the data on breakdown voltages (shown as Paschen curves) for a large number of gases, we show some examples on how these data are coupled with Volt-Ampere (V-A) characteristics, and we proceed to determine secondary electron yields for rare gases (assuming ions to be the primary agent producing secondary electrons) with the inclusion of the effects of equilibration and proper determination of the ionization growth coefficient.

2 Breakdown voltages and Paschen curves

Breakdown is usually represented by a Paschen curve i.e. dependence of the breakdown V_b voltage on the pd (pressure $p \times$ gap d). Parameter pd is a scaling parameter proportional to the number of collisions over a unit distance. In this respect, a typical sharp increase of the breakdown voltage at low pd-s can be explained by the need to compensate for a small number of collisions. On the other hand, at high pd-s, due to a large number of collisions, breakdown voltage is increased in order to enhance energy gain between collisions, when mean free path is getting shorter and the energy gained between two collisions becomes smaller. In the range of the Paschen minimum, production of charges by ionization and secondary electron emission and losses by attachment, diffusion and drift are well balanced.

In Figure 1 Paschen curves for several atomic and molecular gases are presented. Measurements with H_2, SF_6, CF_4, H_2O and C_2H_5OH vapours are taken with the copper cathode, with 1 cm electrode gap and 5.4 cm diameter [10,11]. For all other gases, stainless steel cathode was used in measurements in 2.9 cm gap and 8 cm electrode diameter [6,12]. Some of the data had preliminary presentation in the second edition of the textbook by Lieberman and Lichtenberg [13].

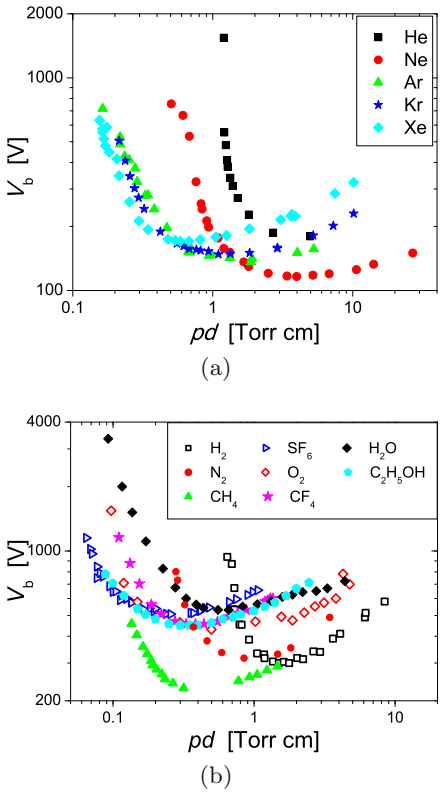

Fig. 1. Paschen curves for (a) atomic gases: Ar, He, Ne, Xe, Kr [6] and (b) molecular gases H_2, SF_6, O_2, CH_4, N_2 [12], CF_4 [10], and H_2O [11] and C_2H_5OH vapours. Measurements with H_2, SF_6, CF_4, H_2O and C_2H_5OH vapours were obtained with copper cathode, for other gases stainless steel cathode was used.

For most of the gases Paschen minimum is situated at pd of the order of 1 Torr cm and breakdown voltages are of the order of several hundred volts. In the case of electronegative gases, it is usually shifted towards smaller pd-s and higher voltages. This can be understood from the point of view of the balance of production and losses of charged particles. In electronegative gases, at low E/N i.e. high pd, attachment becomes important. As a loss mechanism for electrons, it will increase the breakdown voltage and shift the Paschen minimum to lower pressures as an even higher E/N is required to provide sufficient ionization.

There are several issues that one has to be aware of in breakdown measurements. Breakdown voltage depends on the gas mixture through identities of ions and on the cathode material. Even more important than the cathode material is the state of the cathode surface – roughness or possible oxide layers and other impurities deposited on its surface either by exposing the cathode to the laboratory environment or during the discharge operation. Sometimes

the state of the cathode surface has larger influence on the Paschen curve than the material of the cathode itself. For this reason, in our experiments cathode surfaces are treated in low-current (∼30 μA) hydrogen discharge prior to the breakdown measurements. This procedure proved to give stable conditions during measurements and reproducible results over large periods of time. Even when basic breakdown voltage varies due to surface conditions, the Paschen curve (and also the V-A characteristics) maintain their shape and so normalization onto the breakdown voltage is a good way to analyze the data [5,14].

Another issue that has to be taken into account in experiments is the regime in which the discharge ignites. Breakdown voltage should not be confused with the operating voltage. The point where the discharge operates is at the crossing of the circuit load-line and the Volt-Ampere characteristics. Quite often, especially with a small series resistance and sufficiently large overvoltages, this is in the regime of a glow discharge, where voltage can be significantly smaller than the breakdown voltage. Actual breakdown voltage, in the sense that is represented by the Paschen law, can only be found by extrapolating Volt-Ampere characteristics to zero current in the dark Townsend discharge mode. An alternative technique is to study the pre-breakdown currents [15,16]. Sometimes it is even necessary to record the spatial profile of the discharge in order to confirm the exponential increase of emission from the cathode all the way to the anode, which is typical for low-current Townsend discharge.

It is important to emphasize that, besides the Paschen curves, Volt-Ampere characteristics are essential in understanding the process of breakdown. These data are needed to establish the electric field/energy dependence of the secondary electron yields and as a consequence the slope of the V-A characteristics in the Townsend regime is defined. The slope of the characteristics is typically negative in the low-current region and it reveals the ion energy dependence of the secondary electron yield and field distortion due to the initial growth of space charge [2,3,17]. In practice, for a full description of the discharge a 3D plot should be constructed [18], such as the one shown in Figure 2, with discharge voltage (V), pressure × electrode gap product (pd) and discharge current (i) presented at the axes.

Low-current limit represents Paschen curve and in this case it is projected onto 1 μA as further changes of voltage at even lower currents would be negligible. Measurements are taken in a parallel-plate electrode system, with 1 cm gap, 5.4 cm electrode diameter and copper cathode. Considerable difference between the glow regime and Townsend regime voltages is clearly seen from the characteristics.

3 Model of the gas breakdown and secondary electron yields

Secondary electron emission is one of the key mechanisms of DC breakdown and operation of discharges. Still, there

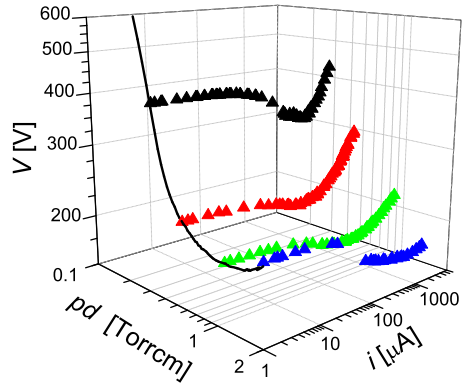

Fig. 2. Experimental V-A-pd characteristics for argon.

is a great confusion in literature in respect to the meaning of the data entering the breakdown condition. In fact, the secondary electron yield data obtained from the gas breakdown have always failed to match the direct measurements in the binary beam-surface experiments. As Phelps and Petrović [5] confirmed in the case of argon, the basic phenomenology of Townsend's theory required extension. Almost constant secondary yield of around 8% for argon ions that has been obtained by ion beams on surfaces cannot be applied to model even the basic low pressure breakdown. While one could justify a greater secondary yield due to additional processes, in the main section of mean energies the yield is actually ten times smaller than that from beam measurements. Phelps and Petrović developed a comprehensive model for argon that included all possible feedback mechanisms – secondary emission by ions, metastables, fast neutrals and photons. They also included back-diffusion of electrons and discussed conditions at the surface where standard gas discharge experiments cannot reach the conditions defined for atomically clean surfaces in ultra-high vacuum. Their study showed that one has to take into account energy dependent yields for each of the species from binary experiments in order to be in accordance with results of direct breakdown measurements. Here, we shall follow the standard procedure to determine secondary yields from the breakdown data and we shall also try to correct some of the problems and provide the data required for such corrections.

Under the conditions of the breakdown and low-current Townsend discharges, the effective secondary emission yield (γ) is related to the ionization coefficient (α) in accordance with the Townsends self-sustaining condition:

$$\gamma = \frac{1}{e^{(\alpha/N)\times Nd} - 1} \tag{1}$$

where N represents the gas number density and d is the gap between the electrodes. $\gamma(E/N)$ may be deduced from Paschen curves by using $\alpha/N(E/N)$ data from the literature [19] as was done in [6]. One may also use an analytic form of $\alpha/N(E/N)$, e.g. Marić et al. [20], as it was shown in [21]. This procedure is the standard one. Perhaps the most important problem in the procedure is that

the non-hydrodynamic region close to the cathode (d_0) affects the total multiplication, and therefore the secondary electron yield obtained from the Paschen curve. The second problem is that the ionization rate taken from the literature may give quite different multiplication as compared with the actual experiment. Even small errors in ionization coefficient result in large discrepancies of the secondary electron yield.

4 Determination of the equilibration distance

It is well-known that hydrodynamic conditions are characterized by transport coefficients that are constant in space and time [22]. However, in low-current electrical discharges at low pressures electrons do not reach the equilibrium state immediately after leaving the cathode. Only at a certain distance from the cathode electrons establish equilibrium with the gas and parameters of electron transport become spatially independent [23,24]. In a simplified approach the width of the non-hydrodynamic region may be used to separate discharge into two regions: one that can be referred to as the non-equilibrium region, with no ionization and the other where ionization behaves as if electrons are in hydrodynamic equilibrium. The problem is then how to determine the delay distance from independent measurements, by using semi-empirical formula such as the one suggested by Phelps and Petrović [5] or by kinetic calculations.

It was shown that inclusion of the effect of equilibration causes a large difference in secondary electron yield data [5], but most authors in the available literature obtain the secondary electron yields from the breakdown data without paying attention to this correction. The role of the equilibration length in determination of the secondary electron yield was studied by Folkard and Haydon [24]. A more detailed discussion of the application of the delay distance and correct determination of the effective electron yield have already been published for the case of argon [6] and for nitrogen [21].

The appropriate form of multiplication factor under Townsend's breakdown conditions is [5]:

$$\gamma = \frac{1}{e^{\alpha(d-d_0)} - 1} \tag{2}$$

where d is the gap between electrodes, and d_0 is the delay distance which has to be passed before electrons reach hydrodynamic equilibrium allowing avalanching characterized by the equilibrium ionization coefficient α. As there is a great need to determine accurate yield coefficients for plasma modeling, there is also a need to establish procedures to determine the equilibration distance.

In our experiments it is possible to obtain equilibration distances from spatial scans of emission. The width of the non-hydrodynamic region d_0 may be used to separate the discharge into two regions. Figure 3 shows two examples of spatial profiles of emission which illustrate the procedure for determination of the equilibration distance and ionization coefficients. In the case of xenon, the non-hydrodynamic width is exhibited as a flat region close to the cathode followed by exponential growth of emission. In the case of neon, there is even a sudden jump of emission just after the equilibration distance. It is still not clear what is the origin of emission in the region next to the cathode [25], as one would expect that there is no emission in non-equilibrium region. Growth of emission in hydrodynamic region is determined by a single exponential that is in excellent agreement with the equilibrium ionization coefficient [26]. While this is not the most accurate method to determine ionization coefficients, it is useful in some situations when the data are lacking and also to indicate the realistic conditions in a particular system which may be affected strongly by the contamination of the gas. Finally, this is the only direct way to obtain total multiplication as required by the breakdown theory.

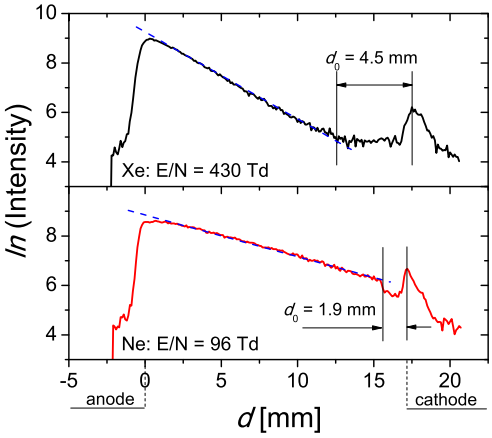

Fig. 3. Examples of the spatial emission profiles in xenon (upper plot) and neon (lower plot), with non-hydrodynamic regions indicated.

When the spatial scans of emission are not available in the experiment that is being analyzed but were available for other experiments, the delay distance d_0 can also be determined by using semi-empirical formulas such as that given in [5] through the expression for the effective value of the electrode potential difference before the exponential growth of the current:

$$V_0 = 16\sqrt{1 + \left(\frac{E/N}{1000}\right)^2}. \tag{3}$$

Probably the best method to produce delay distances is by using Monte Carlo simulations. In this paper we apply a Monte Carlo code that has been well documented in previous publications (details can be found in [27,28]), so only a brief description will be given here. The code is based on generalized null-collision technique [29]. In the code we follow electrons released at the cathode until they reach the anode. The set of cross sections that is used involves inelastic (excitation) processes, ionization and elastic scattering. Each of these processes has associated differential cross sections that are necessary only to establish the angle of scattering. The probability of scattering is determined on the basis of the total cross section. From the simulation of the spatial profile of excitation, one may observe a region

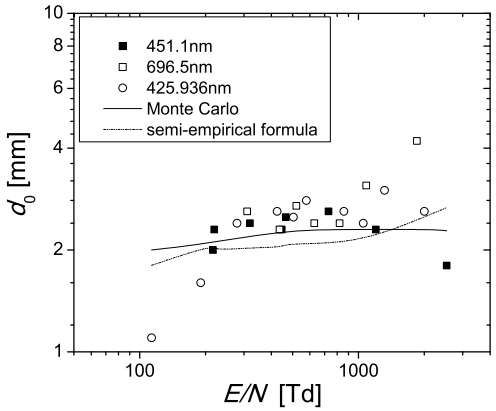

Fig. 4. The dependence of the delay distance d_0 on the reduced field E/N for argon. The delay distances were obtained by three different techniques. Calculations were performed assuming isotropic angular distribution of electrons, the gap between the electrodes of 1.72 cm.

next to the cathode where excitation is zero, followed by an exponential growth of emission and finally a growth with the hydrodynamic ionization coefficient. The hydrodynamic region is extrapolated to the zero value and that point determines the distance as applied in equation (2).

In Figure 4 we compare results for the equilibration distance as a function of the reduced field E/N in argon obtained by experiment (symbols), Monte Carlo simulation (solid line) and semi-empirical formula (dashed line). The results obtained by using three different techniques show good agreement, except for the lowest and highest values of the reduced field. It is necessary to consider here the accuracy of experimental determination of the distance d_0 at those values of E/N. At low values of E/N multiplication is very high and it is not so sensitive on the accuracy of determination of d_0 which is small anyway. On the contrary, at high E/N i.e. low pressures, overall multiplication is small, so inclusion of d_0 does not make significant difference. We may say that the agreement between the experimental data, semi-empirical formula and Monte Carlo simulations is excellent for the purpose of determining the secondary yield coefficients. Still, in experiment, due to reflection from the cathode and scatter of light, the results can be significantly scattered, as it is shown in Figure 4, so for the purpose of determination of secondary electron yields, we use results of Monte Carlo simulations when possible.

While Figure 4 shows results for equilibration distance along the Paschen curve, further on, we explore d_0 behavior for the general non-self-sustained conditions. Pressure dependence of d_0 at a fixed E/N is shown in Figure 5a and the E/N dependence at a fixed pressure in Figure 5b. In both cases, we present the results obtained using our Monte Carlo simulation code (curve) and semi-empirical formula (symbols). For a fixed reduced field, the delay continuously decreases as the gas number density (pressure) increases. On the other hand, the E/N dependence of the equilibration distance for a fixed gas number density (pressure) shows that the equilibration distance becomes

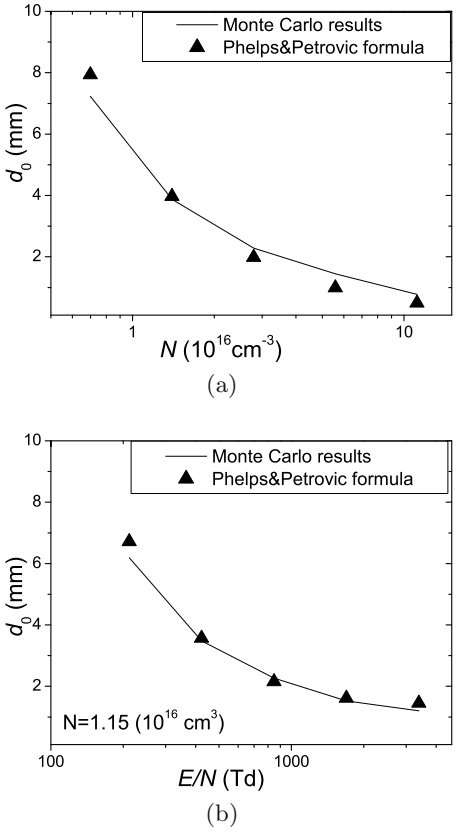

Fig. 5. The dependence of the delay distance on: (a) the gas number density for a fixed reduced field for argon; (b) the reduced field for a fixed gas number density for argon.

smaller as the reduced field increases (for a fixed gas number density). In both cases, the results obtained by semi-empirical formula and the Monte Carlo simulations are in satisfactorily agreement. The experimental measurements are in fact less reliable than the simulation due to limited spatial resolution and possible scattering of light. Thus we really seek a general agreement and put our confidence in simulations. On the contrary, the measured exponential growth, if defined well and if not overlapping with the contribution of fast neutrals, provides better representation of multiplication in the actual experiment. Agreement between results proves that scaling for the equilibration employed in the development of the semi-empirical formula is appropriate.

In Figure 6 we show calculated equilibration distances for different gasses. We have performed analysis mainly for the rare gases and in a limited sense as compared to Phelps and Petrović [5]. Partly, the reason is that experimental determination of the delay distance in molecular gases is very difficult due to several sources of emission and complex quenching. In those gases we recommend Monte Carlo simulation of the whole system both the delay gap and the exponential growth. In Figure 6 it can be seen that the equilibration distance increases with the atomic mass; however it does not change much for a specific gas in the range of E/N-s investigated here.

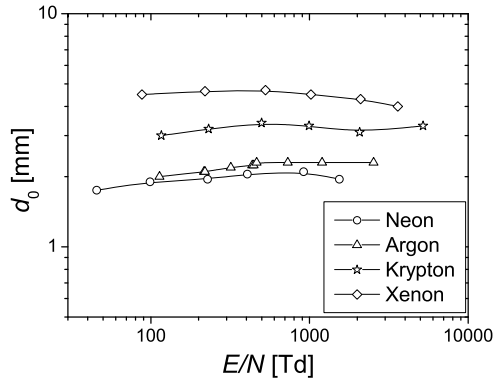

Fig. 6. Equilibration distances for different gases.

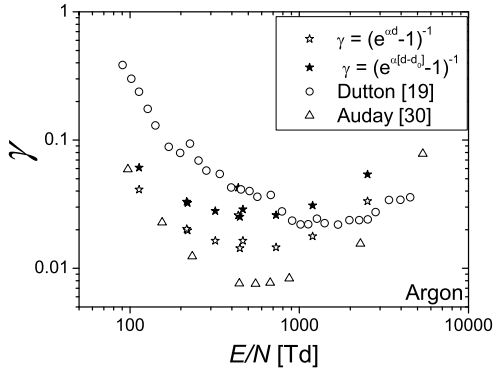

Fig. 7. Comparison of secondary electron yields for argon obtained with different data for ionization coefficients. The first three sets of data were obtained using our Paschen curve, the first two (stars) with our multiplication coefficient without and with the inclusion of the delay distance d_0 in the analysis. The third set (circles) was obtained by using the ionization coefficients from [19] to determine the multiplication. The same ionization coefficients were used in the fourth set [30] but the basis for the results was their measurements of the Paschen curve.

5 Determination of the secondary electron yields and the role of ionization rate

As discussed in previous subsection, the non-hydrodynamic region near the cathode does not necessarily have a significant influence at very low and very high E/N. However, not taking into account the existence of non-equilibrium region can significantly change results for secondary electron yields in medium range of reduced electric fields. In Figure 7 we compare the secondary electron yields in argon obtained by taking into account and not taking into account the equilibration length d_0 (solid and open stars respectively). $\alpha/N(E/N)$ data obtained directly from the experiment are used here to determine γ. As expected, taking equilibration length into account has the largest effect close to the minimum and in the right branch as compared to the left branch. Yet, towards both ends the differences induced by including d_0 diminish. The largest difference between the secondary yields with and without d_0 is a factor of two and it coincides with the minimum of the Paschen curve.

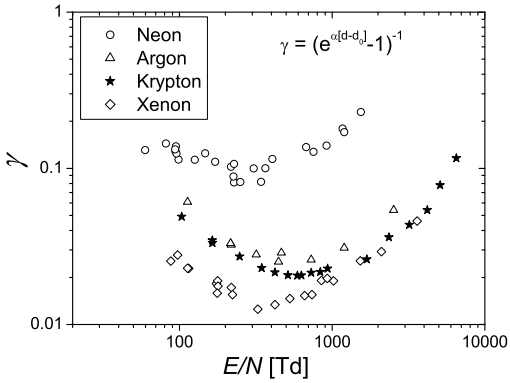

Fig. 8. Secondary electron yields for several different gasses, with the same cathode surface (stainless steel).

Taking the ionization rate from the literature may give a quite different multiplication as compared with the actual experiment and even small errors in the ionization coefficient result in large discrepancies of the secondary electron yield. In Figure 7 we also show secondary electron yields obtained from our Paschen curves by using ionization coefficients from the review [19] which are mostly based on experiments of Kruithiof (circles). These results are up to a factor of 10 different from our data mostly at high E/N.

We also show results of Auday et al. [30] who have analyzed their Paschen curve with the ionization rates from Dutton (triangles). Although those two sets of Paschen curves are apparently quite similar, the differences of yields are considerable, as large as a factor of 10.

For the low values of E/N, γ in our experiment rises more strongly than those obtained by using values of α/N from the literature. This can be explained by the fact that secondary emission of electrons can be due to any combination of numerous mechanisms of varying importance depending on the value of E/N. In the case of small values of E/N, dominant mechanism is the photoelectron emission.

Finally, a similar analysis for the secondary electron yields has been carried out for several other gases. In Figure 8 we show only final results obtained by using the most complete (correct) procedure. As expected the yield increases presumably proportional to potentials of the ion and the metastable states.

6 Conclusions

Measurements of properties of low-current discharges which include Paschen curves, Volt-Ampere characteristics and spatial profiles of emission proved to be a fertile basis for modeling of plasmas and discharges. In this paper we gave a short overview of the results of our breakdown studies covering five rare gases and eight molecular gases. We pointed out the most important issues in deducing secondary electron yields from the breakdown and swarm

experiments, compared results obtained by employing different procedures and we presented results for secondary yields for several rare gases obtained by a proper procedure. One should bear in mind that in this analysis the effective coefficients are attached to ion fluxes and a more thorough analysis along the same lines as done by Phelps and Petrović [5] should be performed for all gases together with an analysis of the applicability of the data in higher current discharges.

In conclusion, we may say that the treatment of electron non-equilibrium motion near the cathode includes determination of the delay in reaching the hydrodynamic rates of electron excitation and ionization. The results obtained when the equilibration distance is accounted for allow us to conclude that not taking into account the non-equilibrium region and correct values of ionization coefficients one may make quite large errors in obtaining secondary yields for the relevant particles in the discharge. These differences between the γ coefficients may result in some of the discrepancies between the swarm and the binary collision technique data for γ coefficients, which remains yet to be analyzed.

Monte Carlo simulation provides complete representation of non-equilibrium effect and influence of the electrodes and it is exact representation of breakdown itself, so it should be employed for modeling. A satisfactory agreement between the experimental data and the results obtained using Monte Carlo simulation code and semi-empirical formula proves that our treatment of the electron non-equilibrium behavior close to the cathode is accurate. It also became possible to make more direct comparisons between the secondary electron yields obtained from Paschen's law and from experiments consisting of a beam of ions hitting the surface under high vacuum conditions and separate detailed analyses should be made for all gases that are of interest.

This work was supported by MESTD ON171037 and III41011 projects.

References

1. J.S. Townsend, *The Theory of Ionization of Gases by Collision* (Constable, London, 1910)
2. Z.Lj. Petrović, A.V. Phelps, Phys. Rev. E **47**, 2806 (1993)
3. A.V. Phelps, Z.Lj. Petrović, B.M. Jelenković, Phys. Rev. E **47**, 2825 (1993)
4. Z.Lj. Petrović, A.V. Phelps, Phys. Rev. E **56**, 5920 (1997)
5. A.V. Phelps, Z.Lj. Petrović, Plasma Sources Sci. Technol. **8**, R21 (1999)
6. G. Malović, A. Strinić, S. Živanov, D. Marić, Z.Lj. Petrović, Plasma Sources Sci. Technol. **12**, S1 (2003)
7. L.C. Pitchford, C. Pedoussat, Z. Donko, Plasma Sources Sci. Technol. **8**, B1 (1999)
8. D. Marić, K. Kutasi, G. Malović, Z. Donkó, Z.Lj. Petrović, Eur. Phys. J. D **21**, 73 (2002)
9. D. Marić, P. Hartmann, G. Malović, Z. Donko, Z.Lj. Petrović, J. Phys. D **36**, 2639 (2003)
10. N. Škoro, J. Phys.: Conf. Ser. **399**, 012017 (2012)
11. N. Škoro, D. Marić, G. Malović, W.G. Graham, Z.Lj. Petrović, Phys. Rev. E **84**, 055401(R) (2011)
12. V. Stojanović, J. Božin, Z.Lj. Petrović, B.M. Jelenković, Phys. Rev. A **42**, 4983 (1990)
13. M.A. Lieberman, A.J. Lichtenberg, *Principles of plasma discharges and materials processing*, 2nd edn. (John Wiley & Sons Inc., Hoboken, 2005)
14. I. Stefanović, J. Berndt, D. Marić, V. Šamara, M. Radmilović-Radjenović, Z.Lj. Petrović, E. Kovačvić, J. Winter, Phys. Rev. E **74**, 026406 (2006)
15. R.W. Crompton, J. Dutton, S.C. Haydon, Nature **176**, 1079 (1955)
16. A.N. Prasad, J.D. Craggs, Proc. Phys. Soc. **76**, 223 (1960)
17. M. Nikolić, A. Djordjević, I. Stefanović, S. Vrhovac, Z.Lj. Petrović, IEEE Trans. Plasma Sci. **31**, 717 (2003)
18. V.I. Kolobov, A. Fiala, Phys. Rev. E **50**, 3018 (1994)
19. J. Dutton, J. Phys. Chem. Ref. Data **4**, 727 (1975)
20. D. Marić, M. Radmilović-Rađenović, Z.Lj. Petrović, Eur. Phys. J. D **35**, 313 (2005)
21. V.Lj. Marković, S.R. Gocić, S.N. Stamenković, Z.Lj. Petrović, Eur. Phys. J. Appl. Phys. **30**, 51 (2005)
22. Z.Lj. Petrović, S. Dujko, D. Marić, G. Malović, Ž. Nikitović, O. Šašić, J. Jovanović, V. Stojanović, M. Radmilović-Radjenović, J. Phys. D **42**, 194002 (2009)
23. J. Fletcher, J. Phys. D **18**, 221 (1985)
24. M.A. Folkard, S.C. Haydon, J. Phys. B **6**, 214 (1973)
25. A.V. Phelps, B.M. Jelenković, Phys. Rev. A **38**, 2975 (1988)
26. Z.M. Jelenak, Z.B. Velikić, Z.Lj. Petrović, B.M. Jelenković, Phys. Rev. E **47**, 3566 (1993)
27. V.D. Stojanović, Z.Lj. Petrović, J. Phys. D **31**, 834 (1998)
28. M. Radmilović, Z.Lj. Petrović, Eur. Phys. J. Appl. Phys. **11**, 35 (2000)
29. H.R. Skullerud, J. Phys. D **1**, 1567 (1968)
30. G. Auday, P. Guillot, J. Galy, H. Brunet, J. Appl. Phys. **83**, 5917 (1998)